

Barrel Sagitta Resolution versus Momentum at 2004 H8 Test Beam and Comparison with GEANT4 Simulation

G. Avolio, E. Meoni, A. Policicchio
(*Physics Department, University of Calabria and INFN*)

F. Cerutti, S. Ventura
(*LNF-INFN, Frascati*)

S. Rosati
(*Physics Department, University of Rome "La Sapienza" and INFN*)

D. Rebuzzi
(*Physics Department, University of Pavia and INFN*)

September 26, 2006

Abstract

This note presents the measurements on muon sagitta reconstruction with the ATLAS Muon Barrel Chambers at the H8 Combined Testbeam. The H8 setup gives an unique possibility to measure this quantity in a realistic setup before the installation of the ATLAS experiment. The sagitta resolution of the barrel muon spectrometer has been measured for various muon momenta, thus disentangling the intrinsic resolution term from the multiple scattering contribution. A good agreement of the results with the MDT design performance has been found. The results obtained from the analysis of the data collected during the 2004 test beam have been compared to the prediction of the GEANT4 simulation of the test beam setup.

1 Introduction

An extensive set of tests of the ATLAS Muon Spectrometer has been developed at the H8 beam line at the CERN SPS. The main aim is to test and to validate many aspects of the muon system performance. The setup realized for the test of the summer 2004 reproduced one projective tower of the barrel and one end-cap octant. During the data taking period events with muon energies ranging from 20 GeV to 350 GeV were collected.

Extensive studies could be performed with this setup: mechanical detector installation tests, integration between different technologies of the Spectrometer, the detector control system, integration between different subsystem tasks (trigger and tracking) and different software tools (the data acquisition, databases, high level trigger software, on-line and off-line monitoring and reconstruction, alignment and calibration).

A figure of merit of the Muon Spectrometer performance is the sagitta resolution. The ATLAS Muon Spectrometer has been designed to provide a good stand-alone momentum measurement, the transverse momentum (p_T) should be measured with a resolution of $\Delta p_T/p_T = 10\%$ at $p_T = 1 TeV$. Since a bending of the 1 TeV muon track is such that the sagitta varies between 500 μm in the barrel and 1 mm in the end-cap, the error on the sagitta measurement must be at level of 50 μm . The H8 setup gives an unique possibility to measure this quantity in a realistic setup before the installation of the ATLAS experiment. The measured sagitta resolution depends not only on the intrinsic resolution but also on multiple scattering, an energy scan is needed to disentangle the two contributes. On this purpose, with the 2004 H8 data it was also possible to measure the beam momentum¹.

In the first section the H8 muon setup for the test of 2004 is described. Section 2 explains how the measurements of both momentum and sagitta have been performed. In Section 3 the data sets used have been reported. The results are shown from Section 4, to Section 8. Section 9 describes the GEANT4 simulation for the testbeam used in these studies. In the last Section, the measured sagitta resolution as a function of the measured momentum at three different MDT discriminator thresholds is shown in comparison to simulated data.

2 The H8 Muon Setup for the 2004 Test

The H8 muon beam, with energies ranging from 20 to 350 GeV , is obtained from the proton beam extracted from the SPS CERN accelerator. The upstream section of H8 test area is reserved to Calorimeter and Inner Detector tests, and it is separated from the Muon Spectrometer area by the beam dump, an iron block of 3.2 m thickness.

A schematic top view of the 2004 muon setup is shown in Figure 1, where the two parts, the barrel stand and the end-cap stand are shown.

The analysis described in this note has been performed only on data collected by the detectors of the barrel stand.

The barrel part emulates a barrel sector of the Muon Spectrometer, and it consists of six MDT chambers and six RPC chambers, with the MDT tubes oriented in

¹A beam magnet has been installed between the MDT chambers as described in section 2.

vertical direction (perpendicular to the plane of the Figure 1) and tube layers which are forming with the beam an angle of about 15^0 ($0.26\ rad$).

The MDT chambers are: two inner large (BIL), two middle large (BML) and two outer large (BOL) chambers, installed on three rails. The chambers are fully instrumented with Front End electronics (FE) and readout with the Muon Readout Driver (MROD)[1] and equipped with the optical alignment system.

Each of the middle station MDT chambers has one RPC doublet upstream and another doublet downstream, while the MDT chambers of the outer station have one RPC doublet placed downstream, as foreseen in the layout of the ATLAS Muon Spectrometer [2].

The beam does not illuminate uniformly the two towers of barrel chambers (a tower is composed by : a BIL, a BML and a BOL chamber), and the tower at the top in Figure 1 (that is the one farthest from the control room) is the most illuminated; therefore, only events collected with this tower have been considered in the analysis.

Two additional barrel stations are present on the beam line, upstream the barrel sector: one outer station upstream of the muon wall and one inner barrel on a rotating support (hereafter called rotating BIL). The rotating BIL can rotate around its vertical axis from 0^0 to $\pm 10^0$ respect to the direction normal to beam.

One beam magnet is installed between the rotating BIL and the barrel sector, in order to bend the muon track in the horizontal plane. The magnet current can be controlled remotely in the counting room and varied from $0\ A$ up to $\pm 600\ A$, providing a maximum field integral of about $4\ Tm$.

In the analysis presented in this note, the RPCs are used to perform measurement of the second-coordinate (the vertical coordinate, orthogonal to the precision coordinate measured by the MDT chambers.). Two external trigger systems are available: a small area trigger (SAT), is given by the coincidence of the signals of two scintillators ($10 \times 10\ cm^2$) centred on the beam line, and installed upstream the magnet, while a large area trigger (hodoscope trigger) ($60 \times 100\ cm^2$) is given by the coincidence of the signals of two planes of six scintillating slabs (each of $10 \times 100\ cm^2$). When using the hodoscope trigger, the possibility of vetoing the area covered by the small area trigger is foreseen, in order to veto the higher rate central part of the beam and have a more uniform illumination of the chambers over the whole hodoscope trigger area.

The data on which this analysis has been performed were collected with the barrel chambers and the rotating BIL operated in the same conditions. The gas mixture of MDT chambers was : Ar(93%) and CO_2 (7%) at $3\ bar$ absolute pressure. The high voltage was $3080\ V$. The trigger system was the 10×10 . The data discussed in this note have been collected at three different discriminator thresholds: -36 , -40 , $-44\ mV$. For each threshold a scan of beam momentum has been performed between 100 and $250\ GeV$, by varying the settings of the H8 beam, with these nominal values indicating the beam momentum at the H8 entry, before the Calorimeters and the beam dump. Since the muons in the beam are produced by pions and K mesons in-flight decaying, it is not possible to obtain a perfectly monocromatic beam.

For each group of data at the same beam momentum and at the same threshold, three runs taken in sequence has been selected to perform the analysis:

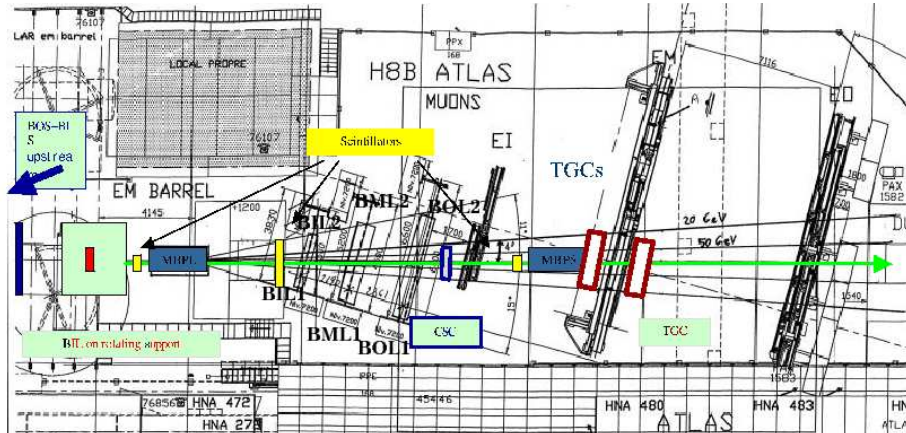


Figure 1: Schematic top view of the 2004 muon setup on the H8 test beam area.

- a run during which the rotating BIL chamber was rotating. This sample is used, as will be explained in section 3, to check the $r(t)$ relation for the MDT gas mixture.
- a run during which the rotating BIL was fixed and the magnet was switched off. This sample has been used to measure the misalignment of the rotating BIL respect to the barrel sector in the $z - x$ plane.
- a run during which the rotating BIL was fixed and the magnet was switched on. This sample has been used to perform both sagitta and momentum measurement.

The analysis has been performed using the package MuonTestBeam of the ATHENA release 10.0.0.

3 Calibration Data

For each tube, the parameters of the raising of the drift time spectrum $t0$, have been derived from a fit to a Fermi-Dirac function. In order to reduce the statistical uncertainties, all the data at a fixed discriminator threshold, used to produce the results of this note, are summed up to compute the fit. Moreover, in order to reduce the electronic noise, a cut on the charge associated to the hit has been applied.

An accurate knowledge of the $r(t)$ relation is necessary to perform the track fit. The standalone C++ software tool, **Calib** [3] has been used to perform autocalibration. For each data set at the same beam momentum and discriminating threshold, the $r(t)$ relations of the two multilayers of the rotating BIL have been measured separately using the runs during which the chamber was rotating.

The same single tube space resolution has been used both in autocalibration and in reconstruction at all thresholds.

The chambers of the barrel sector are kept in fixed position respect to beam axis. Since they are operated in the same conditions as the rotating BIL, the $r(t)$ relation

of the tubes in first multilayer of this chamber has been considered valid also for all the other chambers.

A check on the computed t_0 's and on $r(t)$ relations has been performed investigating the residual distributions separately for each layer as a function of the signed drift distance. The sign separates tracks crossing the tube on the right side of the wire from to ones on the left. The residual distributions of the chambers are shown in Figure 2. The data refer to the run with a nominal momentum of 150 GeV and a discriminating threshold of $-36mV$. The distribution are obtained running the analysis package within the ATHENA framework. No systematic effects are observed.

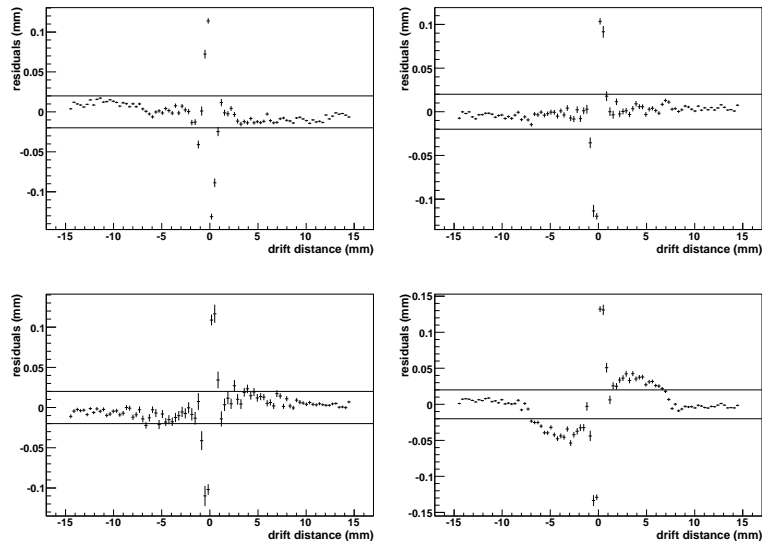


Figure 2: Residual distributions as a function of signed drift distance: for the rotating BIL (top-left), for the BIL (top-right), for the BML (bottom-left), for the BOL (bottom-right).

The large values at small drift distances are due to the difficulty to compute the $r(t)$ relation near the wire. A linear $r(t)$ relation is assumed for radii smaller than 1 mm in this work. The residual distributions of the rotating BIL, of the BIL and the BML are within 20 μm for the overall drift range. Quite larger residuals with an asymmetric behaviour are observed for some data sets in the BOL chamber.

4 The Method to Measure the Sagitta and the Momentum

A schematic top view of the barrel sector is shown in Figure 3, where also the reference system used in the analysis is indicated. The magnetic field and the wires of the MDTs are directed along y -axis (vertical), while the precision coordinate measured by the MDTs is directed along the z -axis (on the horizontal plane $z-x$, orthogonal to the magnetic field). The Rotating BIL chamber measures the angle (ϑ_{RotBIL}) between the x -axis and the muon track upstream of the magnet.

The barrel chambers are measuring the same angle downstream of the field (ϑ_{barrel}). The track is computed as the line that joins the two super-points associated to the track segments separately in the BIL and BOL chambers, where the super-point is calculated as the crossing point of the track segment, reconstructed through a linear fit of the chamber's hit, at the centre of the chamber. The difference between these two angles ($\Delta\vartheta_B$) allows the measurement of the beam momentum, through the formula:

$$p \text{ (GeV)} = \frac{0.3BL \text{ (Tm)}}{\Delta\vartheta_B \text{ (rad)}} \quad (1)$$

where BL is the bending power of the magnetic field, which is known as a function of the magnet current.

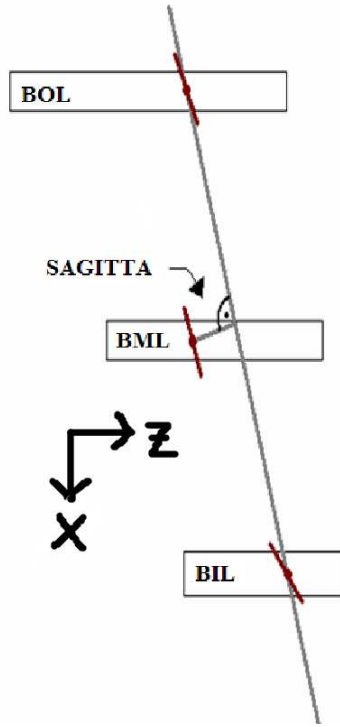


Figure 3: A very schematic top view of the barrel sector in the 2004 muon setup on the H8 area. The figure is not on scale.

As for a given run, the actual orientation of the rotating BIL chamber and the barrel chambers is not known, the measurement of the deflections $\Delta\vartheta_B$ as in 1 has to be repeated with the magnetic field switched off ($\Delta\vartheta_0$).

The final formula is then:

$$p \text{ (GeV)} = \frac{0.3BL \text{ (Tm)}}{(\Delta\vartheta_B - \Delta\vartheta_0) \text{ (rad)}} \quad (2)$$

With this method the muon momentum has been measured using the Muon Spectrometer chambers for the first time. Even if the method is quite different from the one used in ATLAS, it is an important exercise to test the tracking performance of the Spectrometer.

Also the measurement of the sagitta cannot be performed in the same way as in ATLAS, since in the H8 setup the tracks crossing the chambers are straight lines. The track segments are reconstructed separately in each of the three barrel stations (BIL, BML and BOL), the super-points are computed and a straight track joining the two super-points of the two extreme chambers (the BIL and the BOL) is computed (it is the same track used to perform the muon momentum measurement). The sagitta is the distance between the BML super-point and this line.

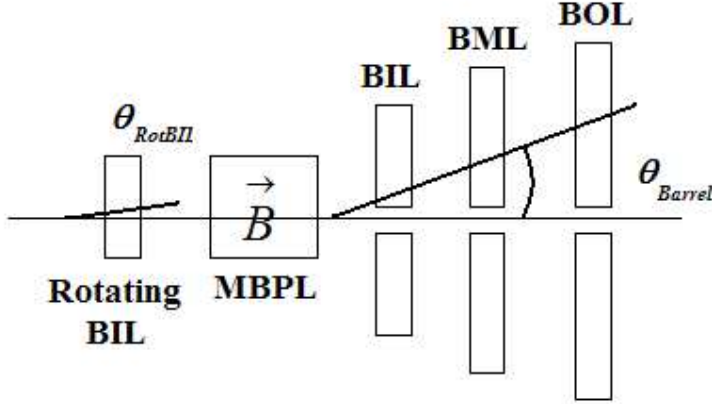


Figure 4: Schematic top view of the muon H8 barrel sector. The method used to measure sagitta is schematized.

As explained in section 2, in H8 setup the barrel chambers are installed on three rails. In the ATLAS Muon Spectrometer, the wires of the different chambers are required to be aligned with a precision of about 2 mrad . A vertical spread of 10 cm , as defined by the small area trigger implies a maximal shift of $200\text{ }\mu\text{m}$ of the wire centres respect to their nominal position in the $z - x$ plane. Then the sagitta and consequently the sagitta resolution depend on the track vertical coordinate. But once this position has been measured with enough precision, the sagitta resolution becomes independent of it. The y -coordinate is measured by the ϕ -strips of the RPCs, that are perpendicular to the MDT wires. Only tracks that cross the BML chamber system at a given value of y -coordinate have been used to compute the sagitta. Figure 5 shows the beam profile for the RPC ϕ -strips of the BML station. The Figure on the left shows the beam profile on the first upstream RPC chamber on both the two ϕ -strip layers. The figure on the right shows the beam profile on the downstream RPC chamber. Due to the geometry setup, the second chamber is more illuminated than the first. The most illuminated ϕ -strip has been selected. It is required at least one hit from this strip in the upstream chamber, and at least one hit from it in second chamber. The results reported in the following sections are obtained after this cut has been applied. It has been checked that equivalent results are obtained if a cut is applied on the RPC ϕ -clusters instead of on the ϕ -strips.

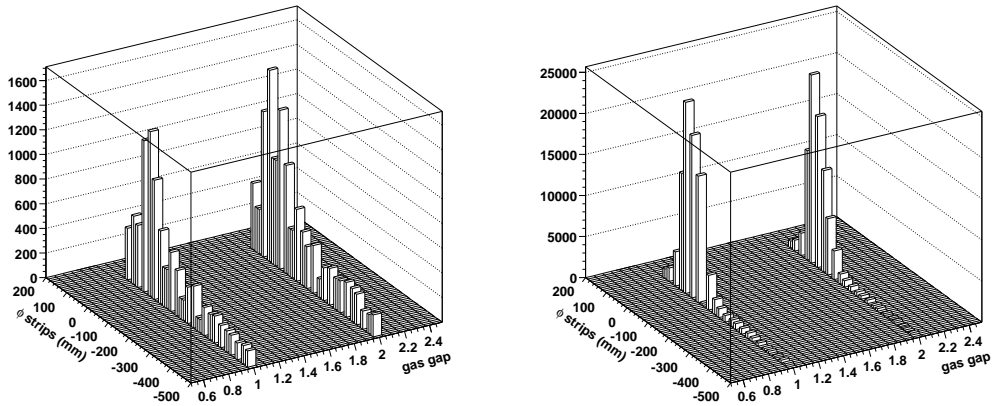


Figure 5: Beam profile on the RPC ϕ -strips of the middle barrel station: on the left the two layers of the first chamber are shown, on the right the layers of the second chamber.

5 Momentum and Sagitta Resolution Measurement

The momentum measurement has been performed as described in section 4. For each beam momentum, first the angular difference $\Delta\vartheta_0$ has been measured to fix misalignment for rotation about the y -axis. Then, $\Delta\vartheta_B$ has been computed. The distributions of the two angular differences are shown in Figure 6 for the runs with 120 GeV nominal beam momentum and -40 mV threshold. Also the measured momentum spectrum, computed with the equation (2), is shown. The measured momentum distributions for all the data sets at the -44 mV threshold, are illustrated in Figure 7. In Table 1 are shown the mean values and the standard deviation of the momentum distributions at the three different threshold, obtained performing a gaussian fit.

Nominal momentum (GeV)	-36 mV		-40 mV		-44 mV	
	p_{mean} (GeV)	σ_p (GeV)	p_{mean} (GeV)	σ_p (GeV)	p_{mean} (GeV)	σ_p (GeV)
100	88.7	4.5	88.8	4.2		
120			108.0	4.2	108.1	4.1
150	136.9	6.1	135.0	5.8	136.1	6.0
180	163.5	7.5			163.4	7.4
220	203.2	11.6	206.7	11.3	202.9	11.5
250	229.4	14.9	230.1	15.1		

Table 1: Measured momentum mean value (p_{mean}) and the standard deviation (σ_p) at different nominal momenta for the three thresholds.

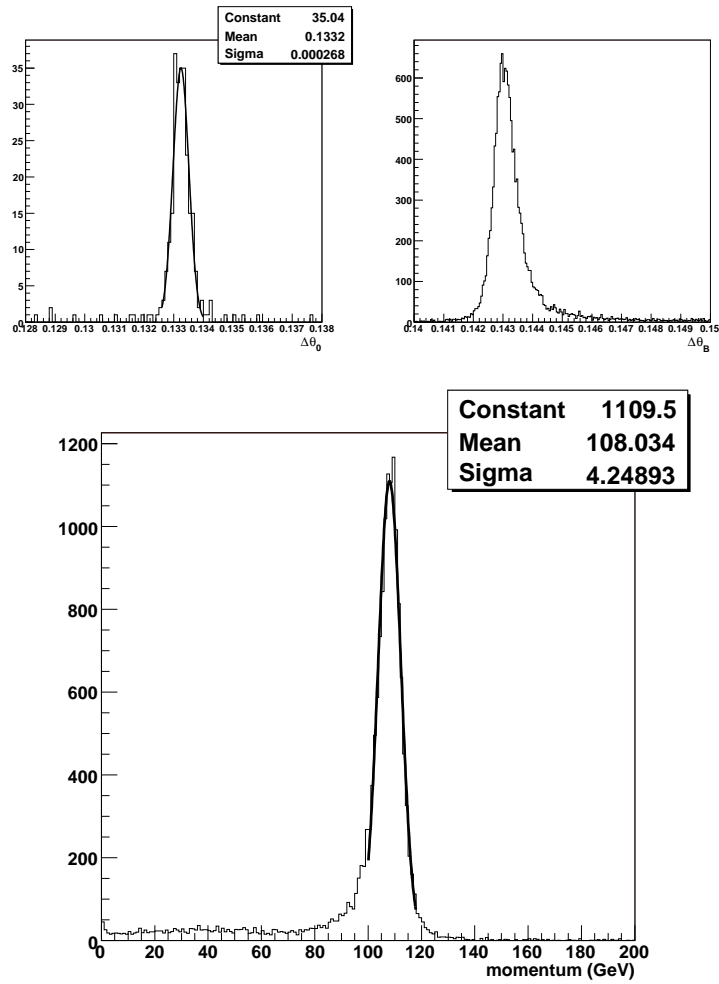


Figure 6: At the top on the left the distribution of $\Delta\theta_0$. At the top on the right the distribution of $\Delta\theta_B$. At the bottom the distribution of the beam momentum. The figures refer to the data set at 120 GeV .

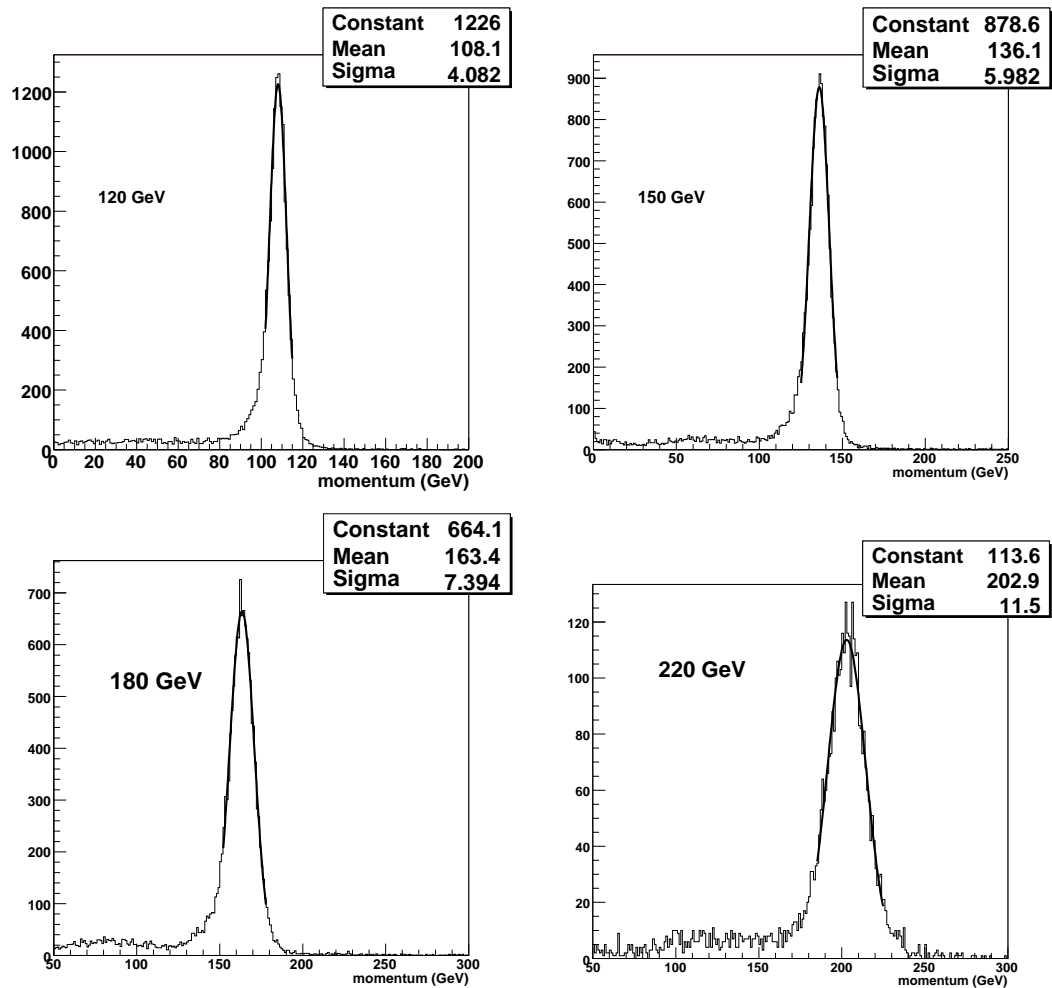


Figure 7: Measured momentum distributions for the different samples at -44 mV threshold.

The difference observed between the nominal and measured momentum are mainly due to the energy loss by the beam in the material upstream the muon area, that is the Calorimeter material and the beam dump.

The sagitta resolution for each data set has been evaluated after two cuts. Only events that pass the RPC cut and with a momentum larger than $p_{mean} - 2\sigma_p$ have been selected. The final sagitta distributions are shown in Figure 8 for the -44 mV threshold. The mean sagitta value and standard deviation obtained with the gaussian fit are reported in Table 2.

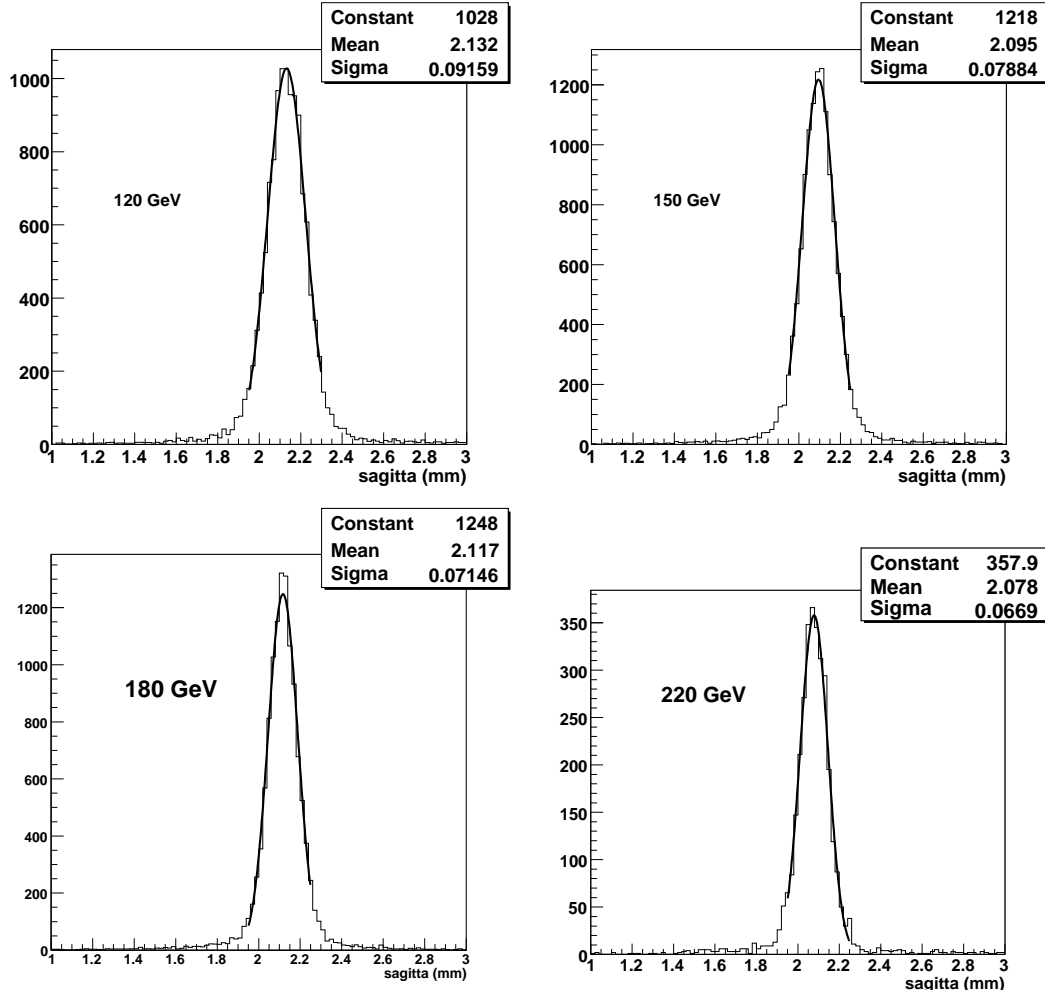


Figure 8: Measured sagitta at different momentum beam after applying constraints described in the text for the -44 mV threshold.

6 The GEANT4 Testbeam Simulation

The simulation of the H8 testbeam has been performed with GEANT4^[4]² running in the ATHENA framework [5] (release 8.8.0). The package CTB_G4Sim³ handles the

²The used version is 06-02-patch01.

³Version CTB_G4Sim-00-02-08, in the cvs repository under offline/Simulation/G4Sim.

Nominal momentum (GeV)	-36 mV	-40 mV	-44 mV
	σ_s (μm)	σ_s (μm)	σ_s (μm)
100	97.99 ± 2.49	101.8 ± 1.1	
120		90.56 ± 0.79	91.59 ± 1.00
150	74.90 ± 1.10	76.46 ± 0.62	78.84 ± 0.82
180	70.15 ± 1.40		71.46 ± 0.71
220	62.99 ± 1.57	65.00 ± 2.00	66.9 ± 1.20
250	59.61 ± 1.96	62.0 ± 1.40	

Table 2: Measured sagitta resolution at different momentum beam after applying the constraints described in the text.

full Combined Testbeam (CTB) simulation, describing in detail the Inner Detector, the LAr and Tile calorimeters and the muon chambers inner structures and positions in the CTB global reference system, as displayed in Figure 9

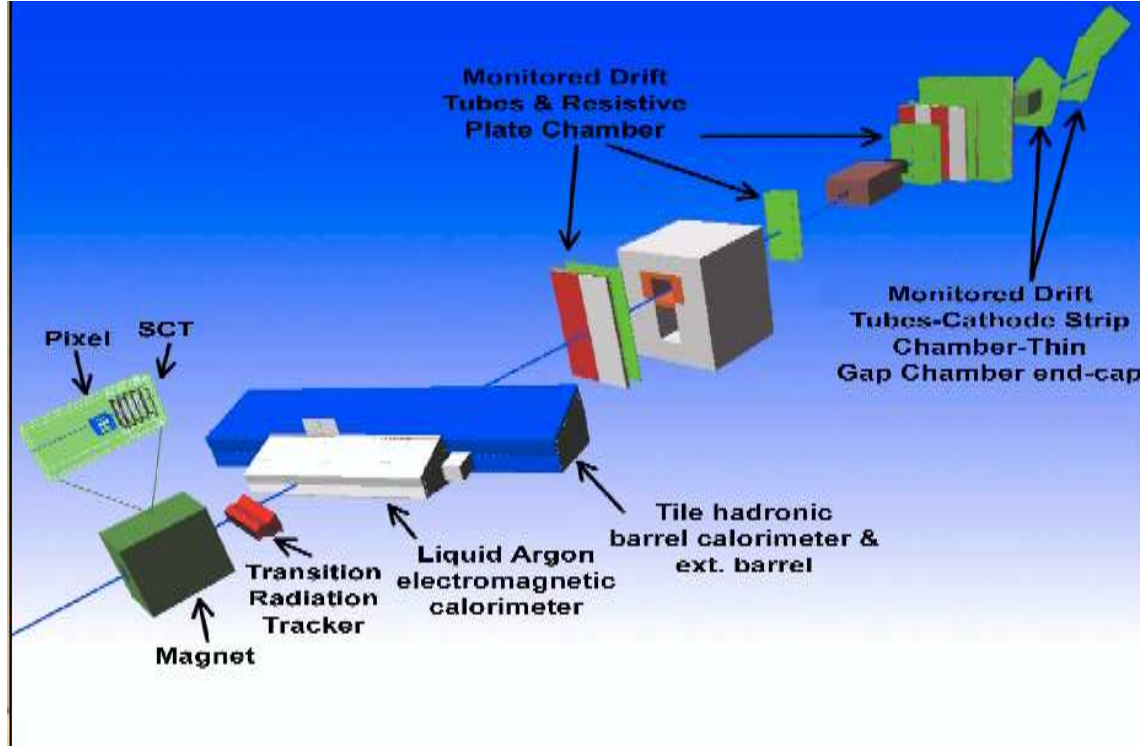


Figure 9: Combined testbeam simulated layout.

The ATHENA SingleParticle generator has been used to produce the muon beam. Beam momentum composition and angular distribution have been tuned on the real data measurements listed in Table 1: in the present simulation, we took advantage of the muon momentum measurements performed using the barrel chambers to realistically describe the muon beam. Any additional detector or dead material upstream the muon sector has been removed from the simulation, this has been estimated the best way to stay close to the real data, avoiding uncertainties coming

from beam interactions with the other subdetectors.

The digitization methods adopted [6] allows to use parametric $r(t)$ relations. Here we chose different resolution curves from the X5 2003 measurements [7], according to the selected discriminator thresholds. The signal propagation along the wire is not considered here. The contribution of this effects to the tube resolution has been estimated to be negligible for the 10×10 trigger runs. As a first check of digitization procedure, we compared data and simulation residuals finding a good agreement, as shown in Figure 10.

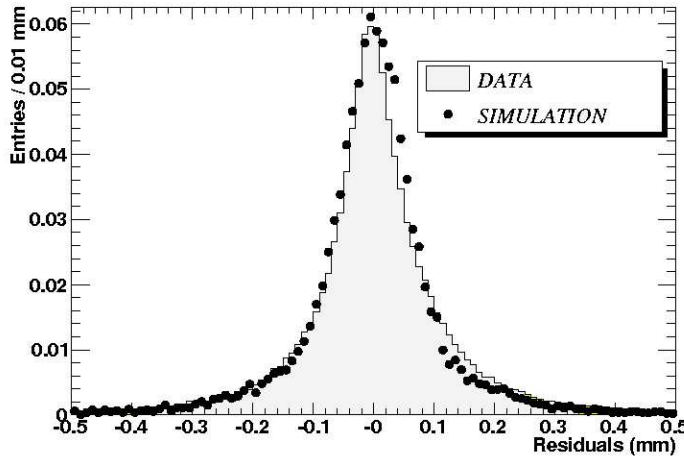


Figure 10: Residuals for real and simulated data.

The simulation is optimized to describe secondary particle production and hard scattering inside the tube, internal tracks and muon hits shielded by secondaries. Our analysis foresaw comparisons at different discriminator thresholds and accordingly, a cut on the energy released by muons in the sensitive gas is applied at the simulation level (respectively, 575eV for the -36mV threshold or 21.3PrimaryElectrons (PE), 640 eV for the -40mV threshold or 24PE, 705eV for the -44mV threshold or 26PE).

The same reconstruction algorithm, MOORE [8], running on the real data samples has been used for the pattern recognition and track fitting performed on simulated data. The same version⁴ of the Detector Description, contained in NOVA database [10], has been used in simulation, digitization and reconstruction.

The simulation comparison with real data is presented in Section 10. Few other tests have been performed to check the sagitta sensitivity to other parameters. For instance, the tube t_0 has been smeared according to a gaussian distribution, with sigma equal to 1, 2 and 3 ns. The intrinsic resolution evaluated from the sagitta width shows a fluctuation from $42 \mu\text{m}$ to $54 \mu\text{m}$ with the increasing t_0 spreading. A 3 ns smearing has a strong impact also on the residuals.

⁴NOVA version 6, corresponding to database amdb a.04 [9].

7 Sagitta Resolution versus Momentum

The three curves of the measured sagitta resolution versus the measured momentum at the different thresholds are shown in Figure 11 for real data using the standard deviation of the sagitta distributions reported in Table 2, and the mean value of the beam momentum reported in Table 1. Figure 12 shows the same curves but obtained with GEANT4.

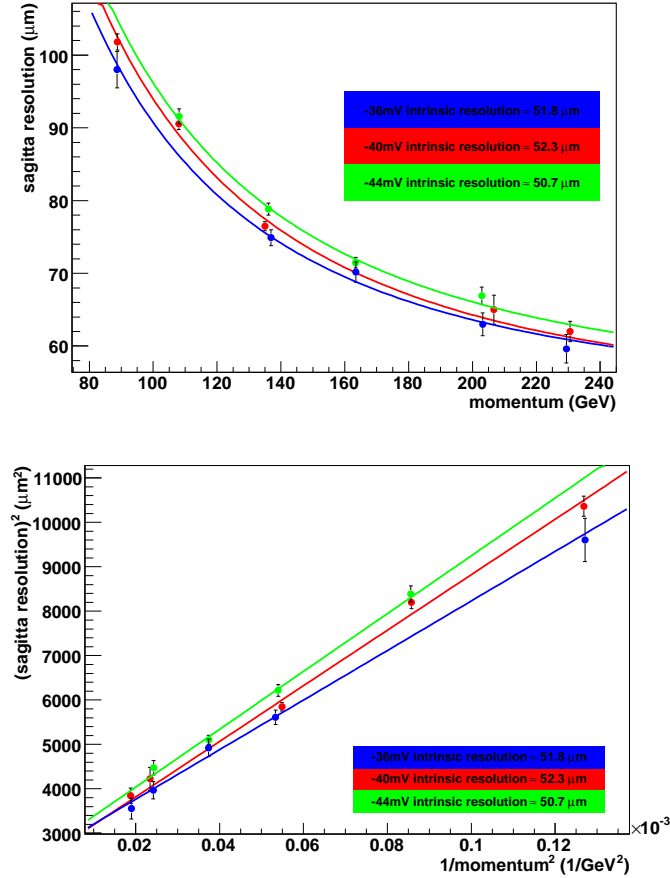


Figure 11: Sagitta resolution as a function of momentum (top) and as a function of $1/p$ (bottom) for real data. The extrapolation and its error when the momentum tends to infinity are immediate in the bottom plot.

The measured sagitta resolution depends mainly on two independent terms: the intrinsic resolution, that is a constant term independent from beam momentum, and the multiple scattering, that depends on muon momentum. The points of Figures 11 and 12 have been fitted with equation (3):

$$\sigma = \sqrt{P_1^2 + (P_2/p)^2} \quad (3)$$

P_1 is the constant term related to intrinsic resolution, P_2 is the term related to multiple scattering.

The term of intrinsic resolution obtained from the fit at the different thresholds for both real data and simulated data are reported in Table 3.

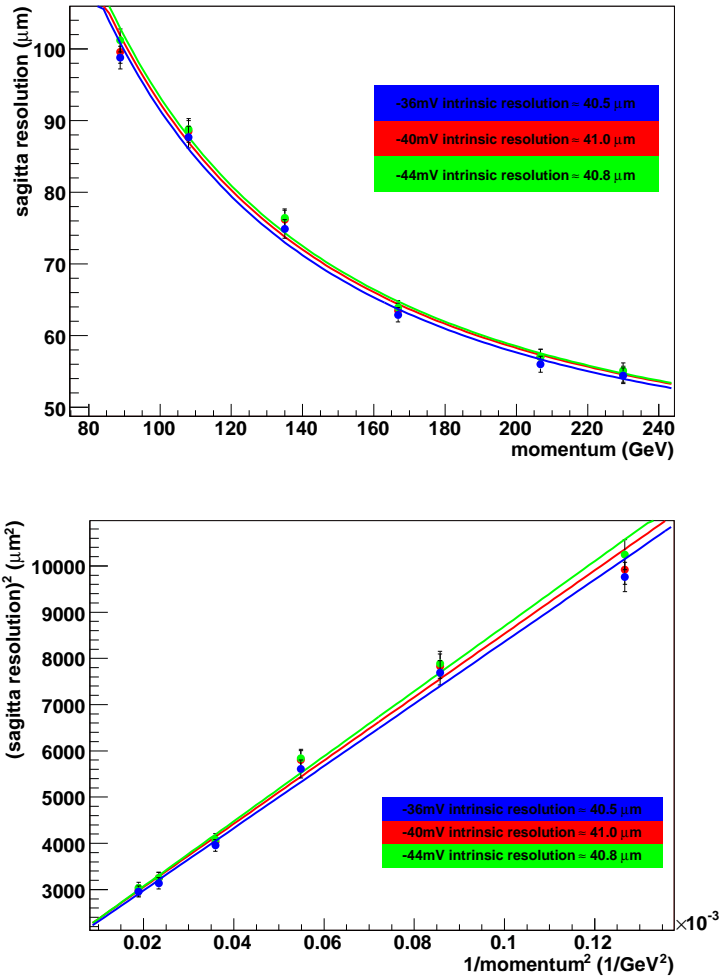


Figure 12: Sagitta resolution as a function of momentum resolution (top) and as a function of $1/p$ (bottom) for simulated data.

Threshold (mV)	Intrinsic sagitta resolution Real Data (μm)	Intrinsic sagitta resolution Simulated data (μm)
-36	51.8 ± 1.9	40.5 ± 1.4
-40	50.7 ± 1.5	41.0 ± 1.4
-44	52.3 ± 1.7	40.8 ± 1.4

Table 3: Intrinsic sagitta resolution values obtained by fit at the different thresholds both for real data and simulated data.

The P_2 term can be translated into the term $\langle x/X_0 \rangle$ that is the average thickness crossed by the track in radiation length units. The schematization reported in Figure 13 has been used to perform the calculation. It has been supposed the scattering happens exactly in the BML super-point. The sagitta resolution term

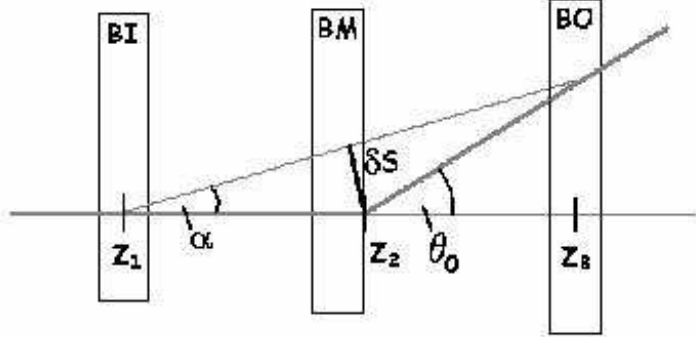


Figure 13: A top schematic view of the barrel chambers. The method to evaluate the multiple scattering contribute to sagitta resolution is schematized.

related to multiple scattering is given by the formula :

$$\sigma_s(\text{multiple scatt}) = \frac{P_2}{p} \simeq \frac{(Z_2 - Z_1)(Z_3 - Z_2)}{(Z_3 - Z_1)} \sigma_{\theta_0} \quad (4)$$

where $(Z_2 - Z_1)$, $(Z_3 - Z_2)$ and $(Z_3 - Z_1)$ are the known distances between the chambers, σ_{θ_0} is the r.m.s. of the multiple scattering angle. It is given by the formula [11]:

$$\sigma_{\theta_0}(\text{rad}) = \frac{13.6 \text{ MeV}}{p} \sqrt{x/X_0} [1 + 0.0038 \ln(x/X_0)] \simeq \frac{13.6 \text{ MeV}}{p} \sqrt{x/X_0}. \quad (5)$$

Substituting 5 in 4, the relationship between P_2 and $\langle x/X_0 \rangle$ is given by the following expression:

$$P_2 \simeq \frac{(Z_2 - Z_1)(Z_3 - Z_2)}{(Z_3 - Z_1)} 13.6 \text{ MeV} \sqrt{\langle x/X_0 \rangle} \quad (6)$$

The values of $\langle x/X_0 \rangle$ obtained by the fit both on real data and simulated data are reported in Table 4. This term accounts for about 9 mm of alluminum of MDT tubes and for the material of the two RPC chambers.

8 Conclusions

In this note a set of results obtained in a full-scale test of the ATLAS Muon Spectrometer, performed in the H8 Test Beam at the Cern SPS, is described. The sagitta resolution as a function of the muon momentum has been measured, for momenta

Threshold	$\langle x/X_0 \rangle$ Real Data	$\langle x/X_0 \rangle$ Simulated data
-36	26.1 ± 2.1	31.5 ± 1.9
-40	29.3 ± 1.0	32.2 ± 2.0
-44	30.5 ± 1.7	33.0 ± 1.2

Table 4: $\langle x/X_0 \rangle$ values obtained by fit at the different thresholds both for real data and simulated data.

ranging from 100 GeV to 250 GeV, and for various electronics thresholds setup of the precision tracking detectors MDT. The beam momentum was measured at the entrance of the barrel muon spectrometer sector, to account for energy losses in the upstream material, and remove tails in the beam energy distributions.

The sagitta resolution has then been measured as a function of the muon momentum, allowing thus to disentangle the two contributions coming respectively from multiple scattering and intrinsic resolution of the tracking detectors. These two terms measured on the test beam data have been compared with the results obtained with the G4 simulation of the H8 setup. The ATLAS offline framework Athena was used for both reconstruction and simulation.

The good agreement found constitutes an important validation of the Spectrometer simulation, in terms of detector materials description and detector response modeling (digitization). An intrinsic sagitta resolution of $50.7 \pm 1.5 \mu\text{m}$ (for an MDT threshold of -40 mV) has been measured, well matching the MDT design performance.

References

- [1] M. Barisonzi et al., *The MROD: the read out driver for the ATLAS MDT muon precision chambers*, 8th Workshop on Electronics for LHC Experiments Electronics for LHC Experiments , Colmar, France , 9 - 13 Sep 2002 - pages 294-295.
- [2] ATLAS Muon Collaboration, *Muon Spectrometer Technical Design Report*, CERN/LHCC 97-22, June 2002.
- [3] P. Bagnaia et al, *CALIB: a Package for MDT Calibration Studies*, ATL-MUON-2005-013, 28-01-2002.
- [4] A. Agostinelli et al, *GEANT4 - a simulation toolkit*, Nucl. Inst. Meth. **A 506** (2003), 250-303.
- [5] ATHENA Developer Guide, http://atlas.web.cern.ch/Atlas/GROUPS/SOFTQARE/00/architecture/.General/Tech.Doc/Manual/2.0.0_DRAFT/AthenaUserGuide/pdf
- [6] D. Rebuzzi, K. A. Assamagan, A. Di Simone, N. Van Eldik, Y. Hasegawa, *GEANT4 Muon Digitization in the ATHENA FRAMEWORK*, ATLAS-COM-MUON-2006-003.

- [7] M. Cirilli et al, *Results from the 2003 beam test of a MDT BIL chamber : systematic uncertainties on the TDC spectrum parameters and on the space-time relation*, ATL-MUON-2004-028, 28-12-2004.
- [8] D. Adams et al, *Track Reconstruction in the ATLAS Muon Spectrometer with MOORE*, ATL-SOFT-2003-007, 02-10-2003.
- [9] AMDB Web Page, http://atlas.web.cern.ch/Atlas/GROUPS/MUON/AMDB_SIMREC/amdb_simrec.html.
- [10] NOVA Parameter Database <http://atlassw1.phy.bnl.gov/NOVA/index.php3>.
- [11] G.R. Lynch, O.I. Dahl, *Approximations to multiple Coulomb scattering*, Nucl. Inst. Meth. B58(1991) 6-10.